

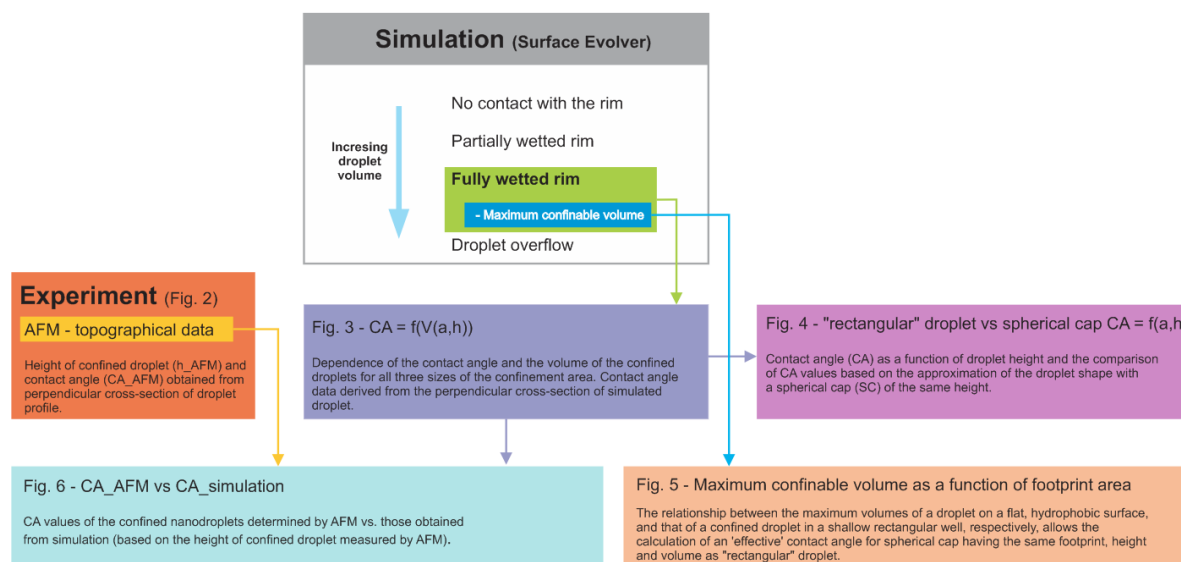
Supporting Information

Confinement of Water Nanodroplets on Rectangular Micro/Nano-arrayed Surfaces

Ondřej Kašpar,^{1,#} Hailong Zhang,^{2,#} Viola Tokárová,¹ Reinhard I. Boysen,² Gemma Rius Suñé,³

Xavier Borrise,³ Francesco Perez-Murano,³ Milton T. W. Hearn,² Dan V. Nicolau,^{1,2,*}

For better understanding the main workflow of this study is shown in **Scheme S1**. Figures 3, 4 and 5 are based purely on simulation results, Figure 6 represents comparison of experimental data - CA_AFM and simulation - CA_sim(h_AFM).



Scheme S1. Experimental and Simulation workflow

S1 Design and fabrication of micro/nano-structured array

The micro-structured arrays were manufactured on $1 \times 1 \text{ cm}^2$ chips cut from P-doped silicon wafers submitted to a dry thermal oxidation process to form a 40 nm thick SiO_2 layer. The chessboard-like organized, $50 \times 50 \mu\text{m}^2$ patterned areas, with squares with the x/y-dimensions of $0.5 \mu\text{m}$ (small), $1 \mu\text{m}$ (medium) and $3 \mu\text{m}$ (large), were defined by e-beam lithography and two different post-processing sequences (described in **Figure S1**), resulting in three types of structures: A, B, and C (**Table S1**).

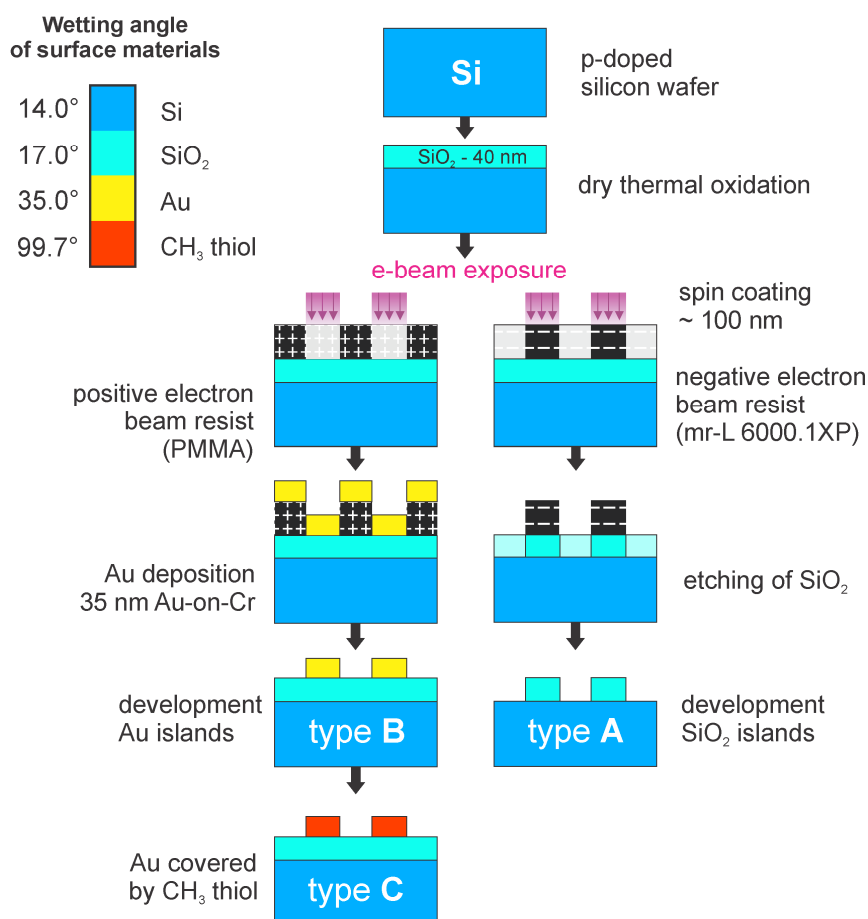


Figure S1. Step-by-step fabrication of droplet confining structures

Table S1. Heterogeneous structures - combination of top and basal substrates

Basal \ Top	SiO₂ (17°)	Au (35°)	CH₃ thiol (99.7°)
Si/ SiO₂ (14 - 17°)	Type A	Type B	Type C

Note: The contact angle of materials is indicated in the top row and left column, for the top and basal materials, respectively.

S1.1 Structure Type A (SiO₂-on-Si)

A 100 nm thick layer of a negative electron beam resist (mr-L 6000.1XP from MicroResist Technology GmbH, Germany) was deposited by spin coating on top of the oxidized silicon chip and then subjected to e-beam lithography. After development, the remaining cross-linked resist serves as a mask for the SiO₂ etching. Wet etching was performed by immersing the chip in a buffered HF solution (SiO₂ etching solution, Merck, Germany) for 20 sec. to selectively etch 40 nm of SiO₂ layer. After the wet etching the resist was eliminated by pyrolysis at 600 °C in the O₂ environment for 5 minutes. The process has been fully described and characterized elsewhere.^[1]

S1.2 Structure Type B (Au-on-SiO₂)

A 100 nm thick layer of a positive electron beam lithography resist (poly-methyl methacrylate, PMMA 950k) was deposited by spin coating on top of the oxidized silicon chip and then subjected to e-beam lithography and development to locally remove the PMMA to form a chessboard pattern; a 35nm thick gold-on-chromium (30 nm/5 nm) layer was deposited over the whole chip

by e-beam evaporation; the remainder of PMMA was removed with acetone resulting in an oxidized silicon surface interrupted by gold protrusions.

S1.3 Structure Type C (CH₃ thiol-on-Si)

The structures Type C present bare silicon (hydrophilic) as basal layer and methyl-terminated thiol-functionalized Au (hydrophobic) as elevated layer. These structures have been investigated in the greatest detail.

S2 Droplet simulations

The shape of the droplet confined in rectangular wells has been simulated using Surface Evolver, a public domain software.^[2] Surface Evolver program, which has been extensively used to analyze the fluid interface,^[3] calculates the shape of a droplet at equilibrium, through the minimization of the free energy of the system. At the micro-scale, the capillary and surface tension forces are predominant compared with gravity. The equilibrium shape of the droplet has been obtained iteratively from the initial shape, e.g., a box, positioned into a fixed model of the well as showed in **Figure S2a**. The process was divided into a series of individual steps to ensure stable simulations (**Figure S2b-d**). After each iteration step the vertices on the interface were moved to reduce the energy of the system while adhering to set of imposed constraints. Detailed information about the software, syntaxes and principles are available in the Surface Evolver manual.^[4] The contact angle was measured by a public domain software, ImageJ,^[5] with implemented plugin that had been designed especially for the drop shape analysis – DropSnake.^[6]

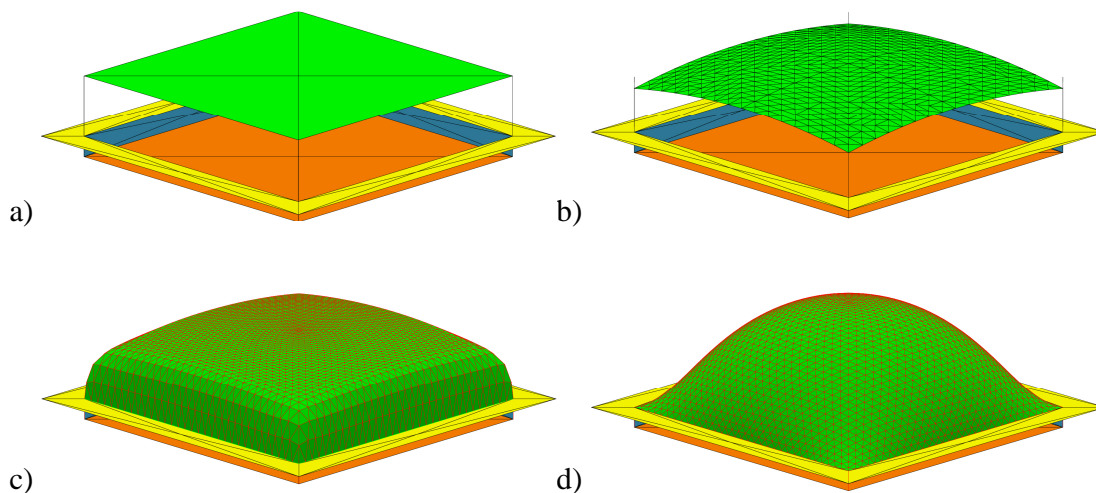


Figure S2. The evolution of the droplet shape in a well Type C (small): a) Initial configuration - green box (dematerialized for better visibility) represents a constant volume of the droplet in the well defined by the bottom (orange) and the walls (dark blue) b) evolution of the droplet in a well of an infinite height c) application of constraints to ensure rim wetting (yellow) d) equiangularity and vertex averaging of the surface has been followed by 2000 iteration steps.

S3 Experimental results

Effect of chemically heterogeneous surface properties

The Type A micro-structured surfaces present only a very small difference between the hydrophilicity of the basal (Si) and top layer (SiO₂), i.e., approximately 3°, which is within the measurement error. Even for this surface, with near-perfect homogenous physico-chemistry, the nm-range topography had a sizable impact on the confinement of the water micro-droplets (**Figure S3a**). While there are small water ‘residues’ on the top surface, essentially all droplets with sizes significantly smaller than the edge of the micro/nano-well are confined within the well, with a clear preference for wetting trilateral surfaces, i.e., corners and edges of the well. The Type

B micro-structured surfaces, with differences between the contact angle for their top and basal surfaces of 21° , induce similar ‘corner wetting’ behavior as the Type A surfaces, but only for larger droplets, i.e., those with a footprint similar with, or larger than the confining rectangular wells (**Figure S3b**). Smaller droplets as confined by smaller wells exhibit a behavior more similar to that observed on micro-structured surfaces with larger differences in local hydrophobicity (Type C). The SAM-modified micro-structures with high differences between the hydrophobicity on the top and on the basal surface induced large differences in the wetting behavior of the water micro-droplets. Specifically, the micro-droplets are nearly perfectly confined on the hydrophilic bottom of the wells surrounded by highly hydrophobic CH_3 -thiol functionalized terminated Au walls (surface Type C, **Figure S3c**). The Type C has been therefore chosen as model chemically- and topographically- heterogeneous structure with ability to confine micro-droplets.

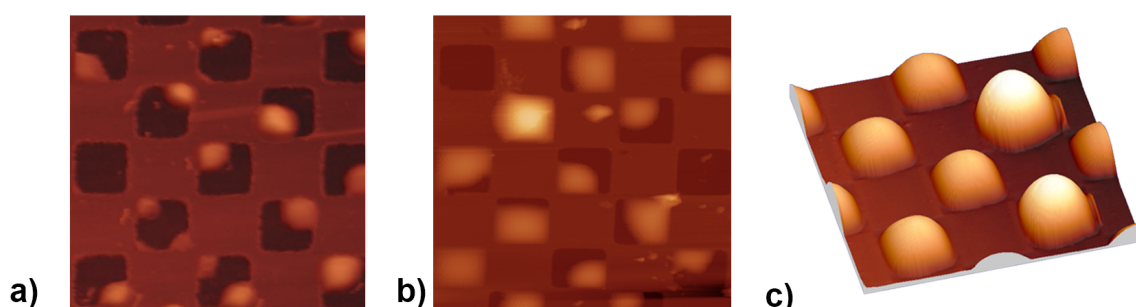


Figure S3. Dependence of the behavior of micro-droplets by spatially addressable hydrophobicity ($3\ \mu\text{m} \times 3\ \mu\text{m}$). The confining topography can ensure the confinement of droplets for nearly-even hydrophilic surfaces (a: Type A), but only for small droplets, which are wetting the corners (low energy configuration). Structures with moderate differences in the local hydrophobicity (b: Type B) shows similar behavior as the Type A, but only for larger droplets. The micro-structures with large differences in the local hydrophobicity, with hydrophilic basal surface and hydrophobic walls and rim (c: Type C) ensure a near-perfect confinement.

Simulation and analysis

It has been shown that in the case of a rectangular well, the stability and shape of a droplet is highly affected by the wall properties, described as Concus-Finn relations.^[7] If the wetting angle θ of the wall in rectangular well is smaller than 45° , the liquid tends to form a wedge and spread along the edges, eventually outside the rim, resulting in poor confinement of the droplet. Condition for capillary self-motion is

$$\theta < \frac{\pi}{2} - \alpha, \quad \text{(Equation S1)}$$

where θ – the Young contact angle on both adjacent planes, α – the wedge half-angle (for rectangular well $\alpha = \pi/4$). On the other hand, if the contact angle is higher than 135° , the droplet detaches and the edge is no longer wetted:

$$\theta > \frac{\pi}{2} + \alpha. \quad \text{(Equation S2)}$$

According to the Concus-Finn relation in the case of well Type A, and B droplet preferably wets corners. If the gravity force is neglected, the droplet has tendency to rise along the edges of the well and spread on the hydrophilic rim. The near-perfect confinement properties of the well Type C (**Figure S3b**) was further rigorously studied by the Surface Evolver software. The example of a steady droplet for the well Type C is shown in **Figure S4**.

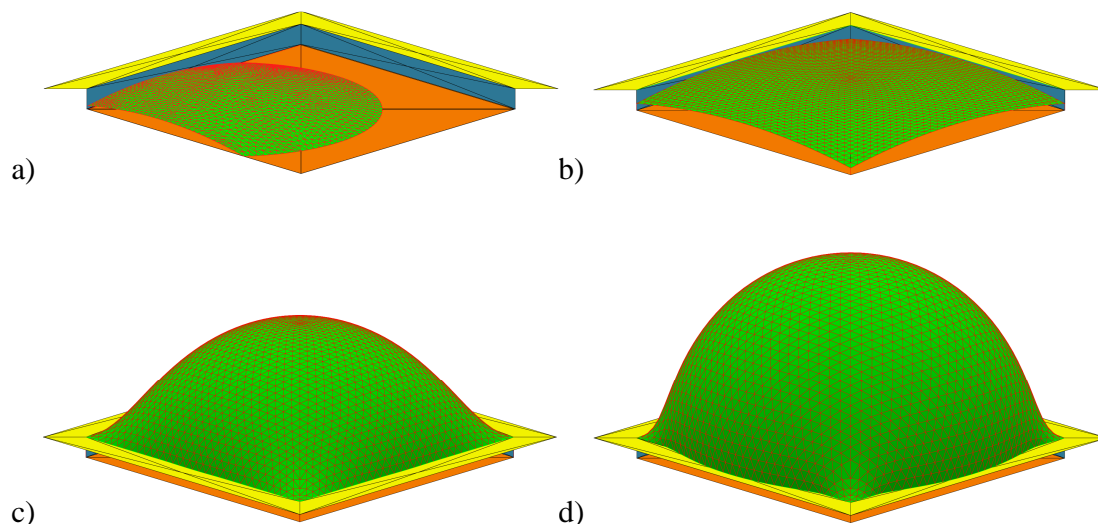


Figure S4. Droplet volume vs. shape for the well Type C (small); a) wetting of one bottom corner; b) complete bottom wetting, no contact with the rim (yellow); c) maximal possible volume of the droplet, no wetting of the rim; d) overflow of the liquid on the rim

The droplet of a small volume can either wet one, or more corners of the well, as presented in **Figure S4a**. The position of the contact line depends on a wettability difference between the bottom and the wall of the well. From theory, if $\theta_{\text{wall}} - \theta_{\text{bottom}} > \pi/2$ the contact line merges with the well bottom edge and droplet whole volume sits only on the hydrophilic bottom of the well.^[8] In our case, the difference $\Delta\theta$ for Type C is 82.7° and contact line is therefore located on the wall (**Figure S4a**). Another possible conformation is a small droplet sitting on the bottom of the well without physical contact with the walls. Larger volumes of the droplet causes complete wetting of the bottom, and eventually contact with the rim, as presented in **Figure S4b**. The contact line is pinned from the middle of the edge until the whole rim circumference is in a contact with the droplet surface (**Figure S4c**). Additional volume results in decreasing the curvature radius until the fluid overflows on the rim (**Figure S4d**). This behavior can be explained by the non-uniform

contact angle along the rectangular well. The two main cross-sections were investigated and are presented in **Figure S5**.

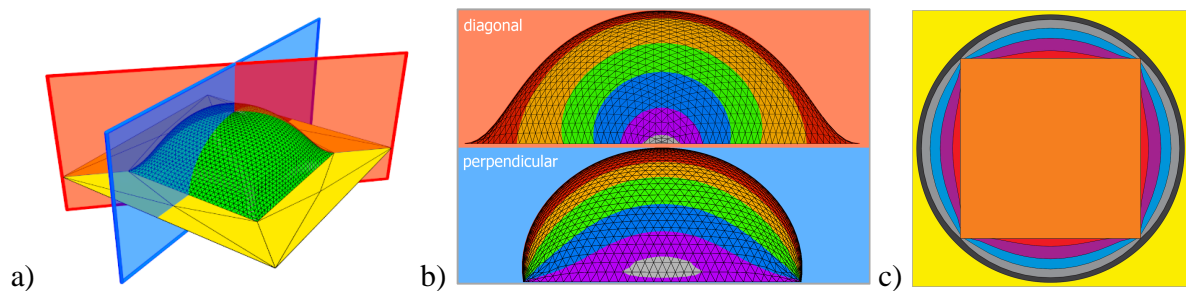


Figure S5. Contact angle variability along the contact line in rectangular well (Type C) – a) 3D visualization - the red plane shows the diagonal cross-section, the blue plane represents the perpendicular cross-section; b) decrease of the droplet curvature radius towards the well corner – red; and towards the rim edge - blue (individual colored areas represent parallel cross-sections); c) bottom view - contact lines of overflowed droplet on the well rim (orange square represents footprint of the well)

The red diagonal cross-section shows inflection point in the proximity of the rim corner and the contact angle is hardly determined. The contact angle value of the droplet in rectangular well was determined from the blue, perpendicular cross-section. Parallel diagonal cross-sections show the decrease of the droplet curvature radius towards the rim corner (**Figure S5b**). This phenomenon causes an increase of the Laplace pressure in the proximity of the rim corner. Liquid is consequently forced to spread towards the center of rim edge and eventually overflows on the top of well rim (**Figure S5c**).

A more detailed relationship between the droplet volume and the contact angle of the rim for well Type C (small) is presented in **Figure S6**. The contact angle shows an exponential growth from its initial value of 9.7° ($99.7^\circ - \pi/2$) to 99.7° . Droplet of very small volume ($V < 7.5$ aL) can either sit on the bottom of the well or in one or more corners as described above. An increase of the volume causes wetting of adjacent walls (blue outline) followed by partial and complete wetting of the rim (green outline). At this point the contact angle between droplet and rim (horizontal plane) can be determined. A further increase of droplet volume leads to increase of the contact angle (CA) value to the point when CA reaches CA of the rim material and no more addition is possible to avoid droplet overflow (red outline). If the maximal confined volume is exceeded droplet overflows on the rim in the middle of rim edge but at the same time remains pinned in the rim corners (black outline) as showed in **Figure S6**.

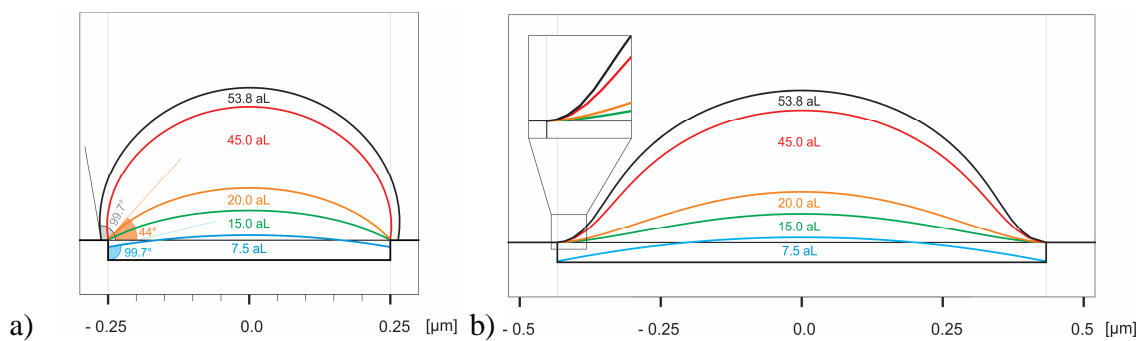


Figure S6. Droplet volume vs. contact angle for well Type C (small) – a) perpendicular cross-section b) diagonal cross-section – zoomed area shows inflection point

The results of the contact angle as a function of a droplet volume measurement are summarized in the **Figure S7**. The “critical” points when the droplet partially or fully wets the rim and when it reaches the maximum and overflow the rim are labelled in different shades of grey.

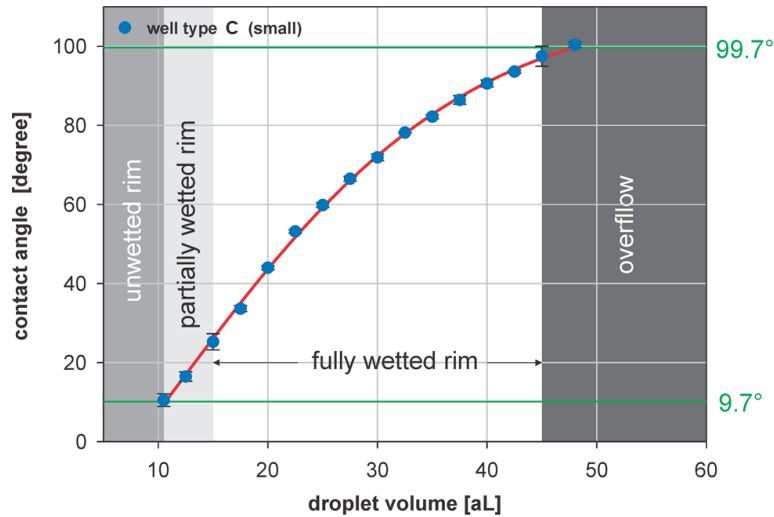


Figure S7. Dependence of contact angle as a function of droplet volume for well Type C (small)

Note: The value of contact angle is determined from the perpendicular cross-section of the simulated droplet shape; the contact angle is measured between droplet and the horizontal rim of the well

The height of confined droplet measured by the AFM was chosen as the most reliable parameter to determine CA value by Surface Evolver simulation. The results obtained from the simulation are shown in **Figure S8**. Dependence of the contact angle on droplet height, for all three size classes of the well Type C, is described by a 3-parametric non-linear regression equation $CA_{sim} = y_0 + a.x^b$, where CA_{sim} is a contact angle obtained from the simulation, x is the height of the droplet and y_0 , a and b are regression coefficients. This equation has been chosen as the best approximation for relatively complex shape of rectangular droplet.

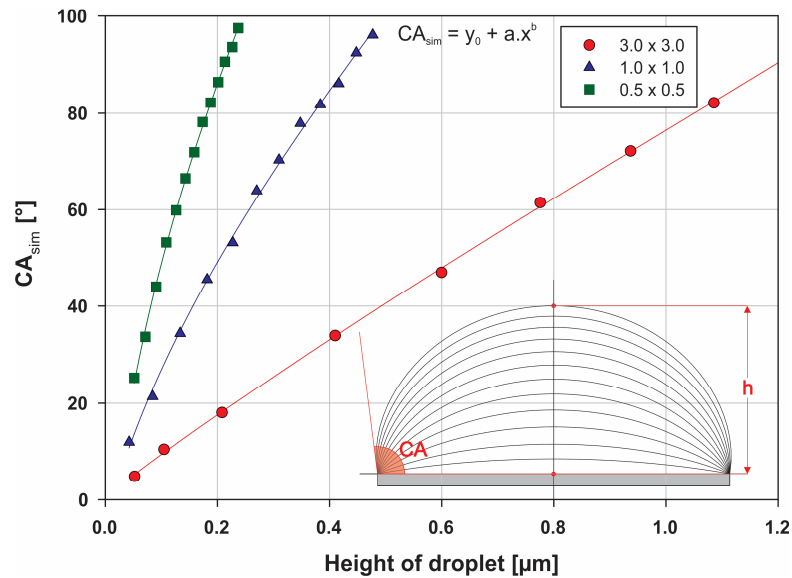


Figure S8. Dependence of the droplet height on CA_{sim} obtained from the simulation (measured in the perpendicular cross-section of the well)

The rectangular character of the footprint results in the non-uniformity contact angle along the rim contact line and affects maximal volume of the confined droplet. Maximal volume of the droplet above the rim (without the base) for circular well with the same footprint area is 1.69-times higher than that of the rectangular one (61.25 aL and 36.25 aL for small C well, respectively) as shown in **Figure S9**.

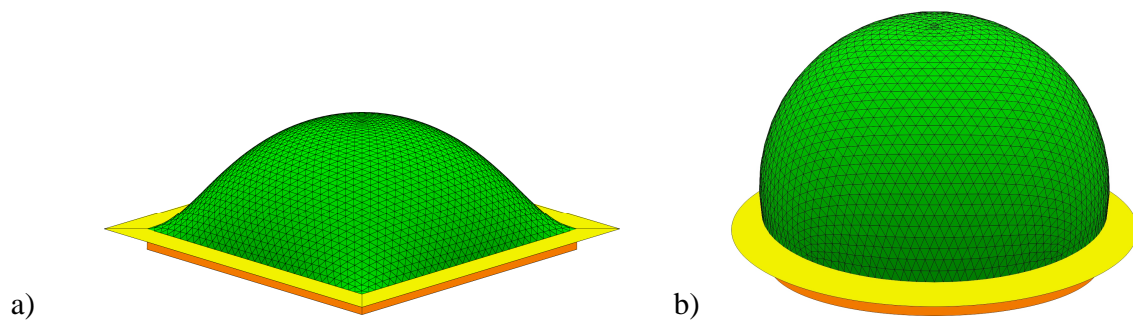


Figure S9. Maximal confined droplet shape and volume for the same footprint area of a) rectangular foot-print (volume of the droplet above the rim - 36.25 aL), b) circular foot-print (volume of the droplet above the rim - 61.25 aL)

References

- [1] C. Martin, G. Rius, A. Llobera, A. Voigt, G. Gruetzner, F. Perez-Murano, *Microelectron Eng* 2007, 84, 1096.
- [2] K. A. Brakke, *Exp Math* 1992 , 1, 141.
- [3] T. H. Chou, S. J. Hong, Y. J. Sheng, H. K. Tsao, *Langmuir* 2012, 28, 5158; Y. Chen, B. He, J. H. Lee, N. A. Patankar, *J Colloid Interf Sci* 2005, 281, 458; S. Brandon, N. Haimovich, E. Yeger, A. Marmur, *J Colloid Interf Sci* 2003, 263, 237.
- [4] K. A. Brakke, *Surface Evolver documentation* 2013, can be found under:
<http://www.susqu.edu/facstaff/b/brakke/evolver>.
- [5] C. A. Schneider, W. S. Rasband, K. W. Eliceiri, *Nat Methods* 2012, 9, 671.
- [6] A. F. Stalder, G. Kulik, D. Sage, L. Barbieri, P. Hoffmann, *Colloid Surface A* 2006, 286, 92.
- [7] P. Concus, R. Finn, *Proceedings of the National Academy of Sciences* 1969, 63, 292.
- [8] K. A. Brakke, *J Geom Anal* 1992, 2, 11.